

The particle fluxes in sediment traps from Niulang Guyot area in the Northwest Pacific Ocean

Xiuwu Sun¹, Jinmin Chen¹, Baohong Chen¹, Cai Lin¹, Yang Liu¹, Jiang Huang², Zhong Pan¹, Kaiwen Zhou¹, Qing He¹, Fangfang Kuang², Hui Lin^{1*}

¹Laboratory of Marine Ecological and Environment Early Warning and Monitoring, Third Institute of Oceanography, Ministry of Natural Resources, Xiamen 361005, China

²Ocean Dynamics Laboratory, Third Institute of Oceanography, Ministry of Natural Resources, Xiamen 361005, China

Received 27 May 2022; accepted 26 August 2022

© Chinese Society for Oceanography and Springer-Verlag GmbH Germany, part of Springer Nature 2022

Abstract

The flux of settling particles in the ocean has been widely explored since 1980s due to its important role in biogenic elements cycling, especially in the transport of particulate organic carbon (POC) in the deep sea. However, research in the seamount area of the oligotrophic subtropical Northwest Pacific Ocean is lacking. In this work, two sediment traps were deployed at the foot and another two at the hillside of Niulang Guyot from August 2017 to July 2018. The magnitude and composition of particle fluxes were measured. The main factors influencing the spatial variations of the fluxes were evaluated. Our results indicated a low particulate flux from Niulang Guyot area in the Northwest Pacific Ocean, reflecting low primary productivity of the oligotrophic ocean. The total mass flux (TMF) decreased from 2.57 g/(m²·a) to 0.56 g/(m²·a) with increasing depth from 600 m to 4 850 m. A clear seasonal pattern of TMF was observed, with higher flux in summer than that in winter. The peak flux of 26.52 mg/(m²·d) occurred in August at 600 m, while the lowest value of 0.07 mg/(m²·d) was shown in February at 4 850 m. The settling particles at the deep layers had similar biochemical composition, with calcium carbonate (CaCO₃) accounting for up to 90%, followed by organic matter and opal, characteristics of Carbonate Ocean. The POC flux decreased more rapidly in the twilight layer because of faster decomposition, remineralization, and higher temperature. A small fraction of POC was transported into the deep ocean by biological pump. Particle fluxes were mainly controlled by the calcareous ballasts besides the primary productivity of the surface water. The advection may be another important factor affecting the flux in the seamount area. The combination of settled matters rich in foraminiferal tests with topography and currents may be the reason for regulating the local abundance of benthos on seamounts. Our results will fill in the knowledge gap of sedimentation flux, improve the understanding of ecosystem in Niulang Guyot area, and eventually provide data support for the optimization of regional ecological modeling.

Key words: sediment trap, flux, seamount, POC, Northwest Pacific Ocean

Citation: Sun Xiuwu, Chen Jinmin, Chen Baohong, Lin Cai, Liu Yang, Huang Jiang, Pan Zhong, Zhou Kaiwen, He Qing, Kuang Fangfang, Lin Hui. 2022. The particle fluxes in sediment traps from Niulang Guyot area in the Northwest Pacific Ocean. *Acta Oceanologica Sinica*, 41(11): 34–44, doi: 10.1007/s13131-022-2106-1

1 Introduction

The export of organic matter from the surface to the deep ocean plays a key role in the global carbon cycle and is a crucial process for the sequestration of atmospheric carbon dioxide (Emerson et al., 1997; Henson et al., 2012; Nowald et al., 2015). It is mainly dominated by a complex ecosystem process “biological pump”, which efficiently and consistently transports a large amounts of carbon molecules in the form of particulate organic carbon (POC) from the epipelagic zone to the deep interior of the ocean and further to the abyssal floor (Honjo et al., 2008). Two major export processes of POC have been identified as gravitational transport by ballasted biogenic amorphous aggregates and active transport by the zooplankton ecosystem. Most sinking POC is remineralized by zooplankton communities to form total CO₂ sinks in the ocean’s interior. These sinks retain CO₂ for a rel-

atively long time (decadal to millennial) compared with epipelagic CO₂ residence time, which is critical in regulating Earth’s climate by preventing runaway accumulation of CO₂ in the atmosphere (Honjo et al., 2008). Thus, only a small fraction of POC reaches the deep sea (Martin et al., 1987). The exported POC can be utilized by seabed-associated community, and its flux becomes one of the main drivers of benthic metabolism (Leduc et al., 2020). In the deep benthos the seasonal changes and inter-annual variation in the species assemblage are highly correlated with POC input (Hernández-Ávila et al., 2021).

The sinking particle flux is estimated by sediment trap and ²³⁴Th/²³⁸U disequilibrium (Ma et al., 2005; Yang et al., 2004). Although the method of ²³⁴Th/²³⁸U disequilibrium, based on the small-volume MnO₂ Co-precipitation technique, is promising for its ease of sampling and high resolution, it has some disadvant-

Foundation item: The Global Change and Air-sea Interaction II Project under contract Nos GASI-04-HYST-01 and GASI-01-NPAC-STsum; the Eastern Pacific Eco-environment Monitoring and Protection Project under contract No. DY135-E2-5-02; the Fund of COMRA-45 Cruise under contract No. DY-HC-135-45; the Scientific Research Foundation of Third Institute of Oceanography, Ministry of Natural Resources of the People’s Republic of China under contract No. 2017014.

*Corresponding author, E-mail: linhui@tio.org.cn

ages, such as uncertainty of the result measured by a single radionuclide (Wei et al., 2015). Furthermore, it is not suited for determining POC flux in deep sea. The time-series sediment trap has great advantages on collecting the settling particles in different periods at different depths regardless of water depth. There were rapidly evolving studies on sediment trap (Buesseler et al., 2008) and time-series studies have been a key tool in understanding the complexities of the biological carbon pump (Ducklow et al., 2009). The sediment trap has been used in the ocean worldwide, such as the Pacific Ocean, Atlantic Ocean (Ramaswamy et al., 1997; Harada et al., 2001; Haskell II et al., 2013; Ran et al., 2015; Kwak et al., 2017; Li et al., 2017; Wilks et al., 2017; Yokoi et al., 2018; Gao et al., 2020). By integrating the data of over 150 traps worldwide over the past 25 a, Honjo et al. (2008) evaluated the export flux of POC (C_{org}) into deep sea and the effect of biological pump, and found that at the depth of 2 000 m, the lowest and highest C_{org} of ~ 25 mmol/(m²·a) and 605 mmol/(m²·a) in the Pacific warm pool and in the Arabian Sea, respectively. Although these studies improved the understanding of the response of the ocean biological pump to climate change, most of them mainly focused on the high productivity areas. The particle fluxes on the subtropical oligotrophic Northwest Pacific Ocean, particularly in seamount area, are poorly explored. The only recent study reported the sinking particle flux from a short-term sediment trap experiment in the subtropical oligotrophic Northwest Pacific Ocean (Kim et al., 2018).

Seamount is one of the main ecological landscapes of oceans. It supports the unique biological communities, with different biological or geochemical properties from off-seamount area (Dower and Mackas, 1996; McClain and Hardy, 2010; Rowden et al., 2010; Priede and Froese, 2013; Turnewitsch et al., 2016). Seamount has become a global hot spot of marine biodiversity, which is, however, scarcely investigated. Only ~ 50 out of 30 000 seamounts have been comprehensively studied in the world (Yesson et al., 2011; Zhang and Xu, 2013).

Niulang Guyot with a flat top and steep slope is located in the subtropical oligotrophic Northwest Pacific Ocean where the southwest and northeast monsoons prevail in summer and winter, respectively. The water depth of the platform is about 1 800 m, with the shallowest part of 1 600 m, and the water depth at the foot is about 5 000 m. According to the topographic characteristics of the mountain, sediment traps at the foot and hillside of the seamount were conducted from August 2017 to July 2018. One-year settling particle flux was measured for the composition and spatiotemporal patterns. The work aimed to provide baselines for carbon cycle, succession of planktonic ecosystem, and seamount benthic ecosystem in typical seamount habitats. It also supports the optimization of regional ecological model. The results would provide insights on biogeochemical particle fluxes in the poorly studied area, and were of great significance for the in-depth understanding of the material cycle of seamount ecosystem.

2 Materials and methods

2.1 Sediment trap samples

Sediment trap moorings were deployed at two sites at Niulang Guyot in the Northwest Pacific Ocean from August 2017 to July 2018. The mooring site MX1 (20.48°N, 160.84°E) is located at the hillside of ~ 2 618 m deep, 71 km east to which is MX2 (20.19°N, 161.45°E) at foot of the seamount of 5 050 m deep (Fig. 1). The MX1 mooring consisted of two automated KUM time-series sediment traps and two sea current meters, attached to a mooring line at 600 m, 2 500 m and 533 m, 2 095 m water depths, respect-

ively. The same instruments were deployed at MX2, but at different water depths of 2 050 m, 4 850 m and 1 845 m, 4 920 m, respectively. Each sampling interval for all deployments was generally 30 d, and each sediment trap was programmed to collect 12 samples. For some reasons, the sample carousel of two sediment traps stopped running (February and March 2018 separately), resulting in missing records of the intervals (Table 1).

Prior to deployment, each 450 mL sample container was filled with artificial seawater containing 35 g/L NaCl and 3.3 g/L HgCl₂ as preservatives (Kwak et al., 2017; Li et al., 2017). After retrieving the traps, the pHs of the samples collected by sediment traps were measured immediately. Then the samples were stored at 4°C in a refrigerator to avoid organic carbon degradation until further laboratory analysis.

2.2 Laboratory analysis

All samples were gently sieved with a 1 mm nylon mesh to remove “swimmers” (any large particles such as swimming and planktonic organisms). Stereomicroscopic analysis indicated that the zooplankton was a negligible constitute of the <1 mm samples. The particles passing through the mesh were split into 8 aliquots using a high precision rotary splitter (FRITSCH, 8 wet sample divider). One of the eight subsamples or “splits” was filtered onto a Millipore polycarbonate membrane filters (0.22 μ m) for biogenic opal analysis. Another five subsamples were filtered on a Sterlitech silver membrane filter (0.45 μ m). The rinsed samples were freeze-dried and then weighed gravimetrically for total mass flux (TMF, mg/(m²·d)) as shown in Eq. (1),

$$TMF = \frac{M}{H \cdot S}, \quad (1)$$

$$F_c = \frac{M \cdot f_c}{H \cdot S}, \quad (2)$$

where M was dry weight mass of the collected sinking particles, S was the cross-sectional collection area of the sediment trap (herein $S=0.5$ m²), H was the sampling time. Fluxes of POC, CaCO₃, and opal were calculated by Eq. (2), where F_c was the flux of a certain component, f_c was the percentage of a certain component in the total mass.

The freeze-dried samples on silver membrane were thoroughly homogenized in an agate mortar to measure carbon and nitrogen contents. The total carbon (TC) content and total nitrogen (TN) content were determined using a Thermo Flash 2000 CNS elemental analyzer with a relative standard deviation of <0.36% and <0.48% based on repeated analysis of a standard material (methionine, Thermo Scientific). A portion of homogenized powder was acidified in acid fumigation instrument with HCl vapor for 3 d to remove carbonate completely. Carbonate-free samples were rinsed to remove HCl and dried for particulate organic carbon content determination. Particulate organic matter (POM) was converted from POC by multiplying the empirical factor of 1.8 (Müller et al., 1986). The particulate inorganic carbon (PIC) content was the difference between TC content and POC content; CaCO₃ content was calculated by multiplying the inorganic carbon content by a conversion factor of 8.33, the ratio of calcium carbonate to carbon's atomic weight.

Biogenic silica (B_{Si}) analysis was performed using a double leaching method by Ragueneau et al. (2005) due to a limited amount of samples, which was less than a required 0.5 g/L solid-liquid ratio of the continuous extraction method. The dry samples were left on polycarbonate membrane in polypropylene

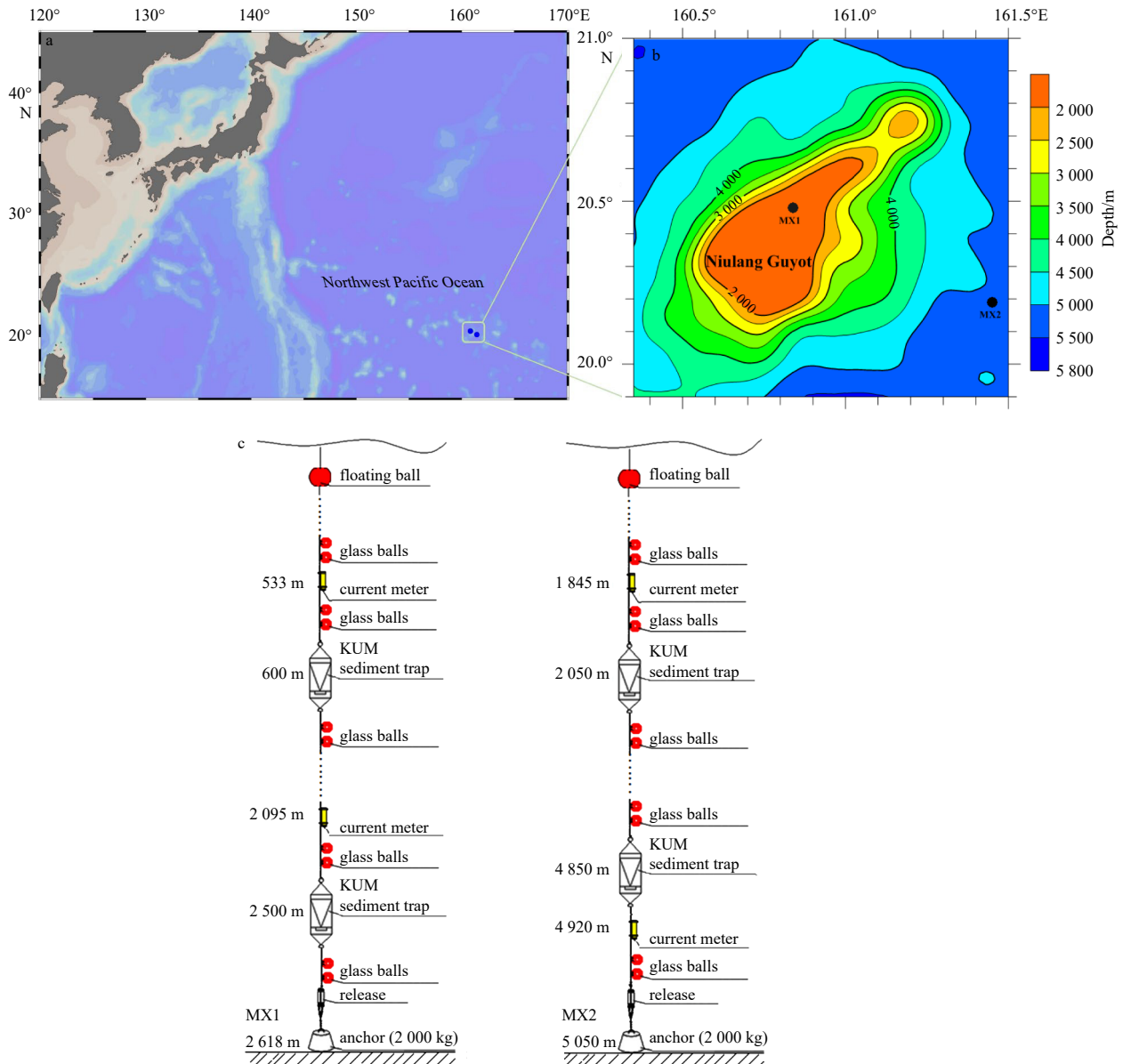


Fig. 1. Location and vertical structure of the mooring systems in Niulang Guyot area. a. Location of Niulang Guyot in the Northwest Pacific Ocean; b. topographic map of Niulang Guyot; c. schematic diagram of two moorings.

Table 1. Sampling information record of sediment traps

Station	Latitude	Longitude	Deployment layer/m	Deployment time	Recovery time	Sample quantitie
MX1	20.48°N	160.84°E	600	2017.08.04	2018.07.25	12
			2 500	2017.08.04	2018.07.25	8
MX2	20.19°N	161.45°E	2 050	2017.08.05	2018.07.26	7
			4 850	2017.08.05	2018.07.26	12

Note: The sample carousel of two sediment traps stopped running (February and March 2018 separately), resulting in missing records of the intervals.

centrifuge tube leached with 0.2 mol/L NaOH at 100°C water bath for 40 min. Then, 1 mol/L HCl was added to neutralize the pH of the cooled extract and centrifuge at 2 500 r/min for 10 min. Afterwards, the supernatant was diluted for the determination of $[Si]_1$ (concentration of silicate in the first extraction solution) and $[Al]_1$ (concentration of aluminum in the first extraction solution). The above steps were repeated for the same sample to obtain $[Si]_2$ (concentration of silicate in the second extraction solution) and $[Al]_2$ (concentration of aluminum in the second extraction solu-

tion). The B_{Si} concentration was calculated with the Eq. (3). The dissolved silicate concentration of the leachate was analyzed with the silicomolybdenum blue method using a spectrophotometer and the Al content was measured with ICP-MS (Agilent 7700x, USA). Opal content was converted from biogenic silica by multiplying the molar mass ratio of 2.4 (Mortlock and Froelich, 1989). Finally, the lithogenic material flux was calculated as the difference of total particle flux and biogenic fluxes ($CaCO_3$, POM and opal).

$$[BSi] = [Si]_1 - [Al]_1 \times \frac{[Si]_2}{[Al]_2} \tag{3}$$

3 Results

3.1 Variations of environmental parameters

Sea surface temperature (SST) varied between 25.4°C and 30.0°C with a mean of 27.9°C. SST was usually higher than 29°C from June to October and lower than 26.5°C from January to May (Table 2, Fig. 2). The concentration of chlorophyll *a* in the surface layer varied from 0.03 mg/m³ to 0.09 mg/m³ with a mean of

0.05 mg/m³ (Fig. 2). It was found that temperature dropped abruptly with depth (Table 2). From the surface layer to about 1 000 m, the temperature decreased from 27.9°C to 4.4°C. At >2 000 m, the temperature dropped from 2.0°C to 1.4°C, with a variation range of from 0.3°C to 0.1°C. Current velocity varied greatly with depth (Figs 3a–d). At 553 m depth, the average current velocity was 10.6 cm/s, which flowed mainly to the northwest, followed by the

Table 2. Characteristic values of temperature (from August 2017 to July 2018)

Depth/m	Temperature/°C		
	Maximum	Minimum	Average
Surface	30.0	25.4	27.9
533	9.5	6.4	7.9
932	4.8	4.1	4.4
1 846	2.4	2.1	2.3
2 086	2.2	1.9	2.0
4 846	1.5	1.4	1.4

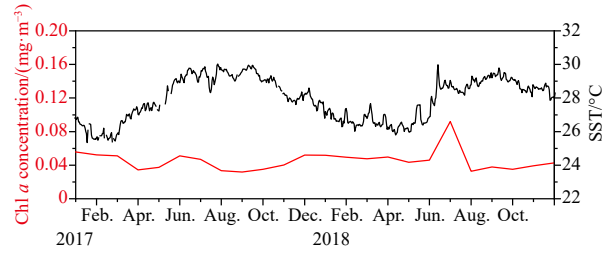


Fig. 2. Seasonal variations of chlorophyll *a* (Chl *a*) concentration and sea surface temperature (SST) from January 2017 to December 2018. The red line was Chl *a* concentration and the black line was SST (data obtained from http://apdrc.soest.hawaii.edu/datadoc/modis_aqua_chla.php and http://apdrc.soest.hawaii.edu/datadoc/oisst_avhrr.php).

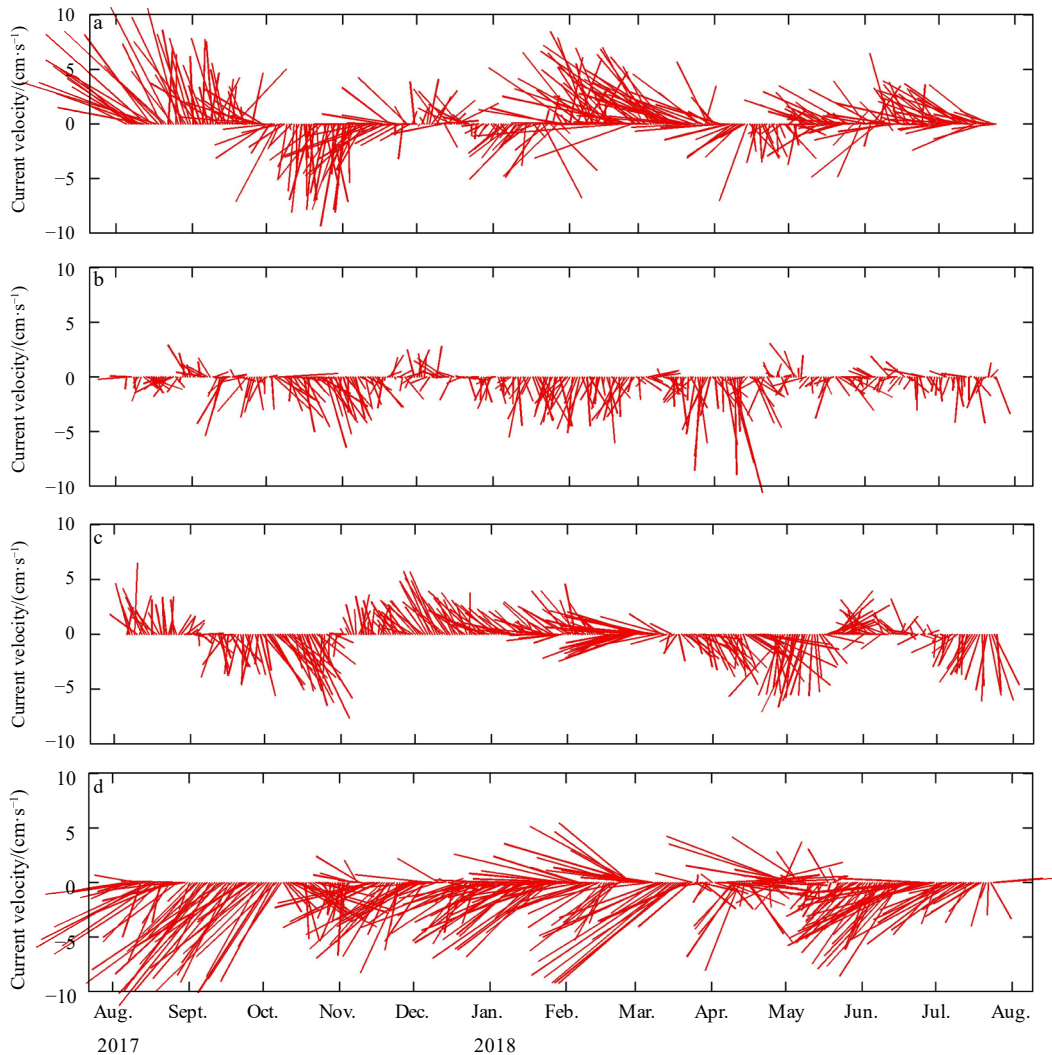


Fig. 3. Current velocity and flow direction of 533 m (a), 2 095 m (b), 1 846 m (c) and 4 920 m (d).

south or southwest. The average current velocity at 2 095 m was about 6.3 cm/s, and it almost flowed to the south all year round. The average current velocity at 1 846 m was 6.0 cm/s, and the flow directions were mainly northwest or southwest, followed by southeast. The current velocity at 4 920 m increased, with an average of 10.1 cm/s, and the flow direction was mainly southwest.

3.2 Settling particle fluxes and their composition

Settling particle fluxes of two sites for the four depths were shown in Fig. 4 and Table 3. The results indicated that the peak of TMF appeared in summer, while the valley occurred in winter. At MX1 site, TMF varied from 3.36 mg/(m²·d) to 26.52 mg/(m²·d) at 600 m deep with a total of 2.57 g/(m²·a). The highest TMF of the whole year appeared in August (Fig. 4a). TMF varied from 0.13 mg/(m²·d) to 3.12 mg/(m²·d) at 2 500 m, with a total of 0.64 g/(m²·a), which was about 75% lower than that of the upper trap (Table 3). At MX2 site, TMF varied from 0.75 mg/(m²·d) to 5.70 mg/(m²·d) at 2 050 m, with a total of 0.70 g/(m²·a), which was about 8% higher than that of at 2 500 m deep (Fig. 4b). For the 4 850 m trap, TMF varied from 0.07 mg/(m²·d) to 6.83 mg/(m²·d) with an annual of 0.56 g/(m²·a), which was about 20% lower than that of at 2 050 m. The lowest TMF of the whole year appeared in February (Fig. 4d). TMF gradually decreased with depth, with a significant decrease in the upper ocean. The extreme fluxes of TC, TN, CaCO₃, and POC were mostly consistent with those of TMF at the same layer.

At 600 m layer of MX1 station, POM content ranged from 10.4% to 39.1%, with a mean of 23.9%. CaCO₃ content varied from 34.0% to 88.7%, with an average of 70.1%. Opal content ranged from 0.17% to 3.8%, with a mean of 1.5%. The sum of POM,

CaCO₃, and opal contents accounted for >95% of the total except in August (Fig. 5a). At 2 500 m layer, POM, CaCO₃, and opal contents ranged from 6.65% to 9.6%, 65.3% to 84.4%, and 1.1% to 11.1%, respectively. The sum of opal, POM, and CaCO₃ contents accounted for up to 96.3% (Fig. 5c). At 2 050 m of MX2, POM, CaCO₃, and opal contents ranged from 6.24% to 14.62%, 52.6% to 84.9%, and 3.3% to 10.8%, respectively. The sum of opal, POM, and CaCO₃ contents accounted for up to 97.0% of total mass (Fig. 5b). At 4 850 m layer, POM, CaCO₃, and opal contents varied from 6.4% to 7.3%, 57% to 90%, and 2.2% to 14.0%, respectively (Fig. 5d). In this area, CaCO₃ contributed most to mass flux of the measured phases (34%–90%), followed by POM (<6.2%–39.1%) and opal (<0.2%–14%), while lithogenic material provided only minor contribution.

4 Discussion

4.1 Composition and change of sedimentation flux

Sinking particles in the ocean mostly consist of biogenic materials (Honjo et al., 1995; Kim et al., 2011, 2014, 2018), including organic matters, CaCO₃, biogenic opal, and ballast. In the subtropical oligotrophic Northwest Pacific Ocean (SONP), CaCO₃ content is between 50% and 90%, and POC is up to 20% (Kemp and Knaack, 1996; Mohiuddin et al., 2002; Kim et al., 2011, 2018). Our results were in good agreement with previous study. POC content was significantly correlated with TN content ($r=0.77$, $P<0.01$) and POC/TN content ratio was lower than 8, indicating POM was mainly derived from marine authigenic organic matter. POC content was not related to B_{Si} content, indicating diatoms didn't play a major role in POC transport. The Carbonate Ocean

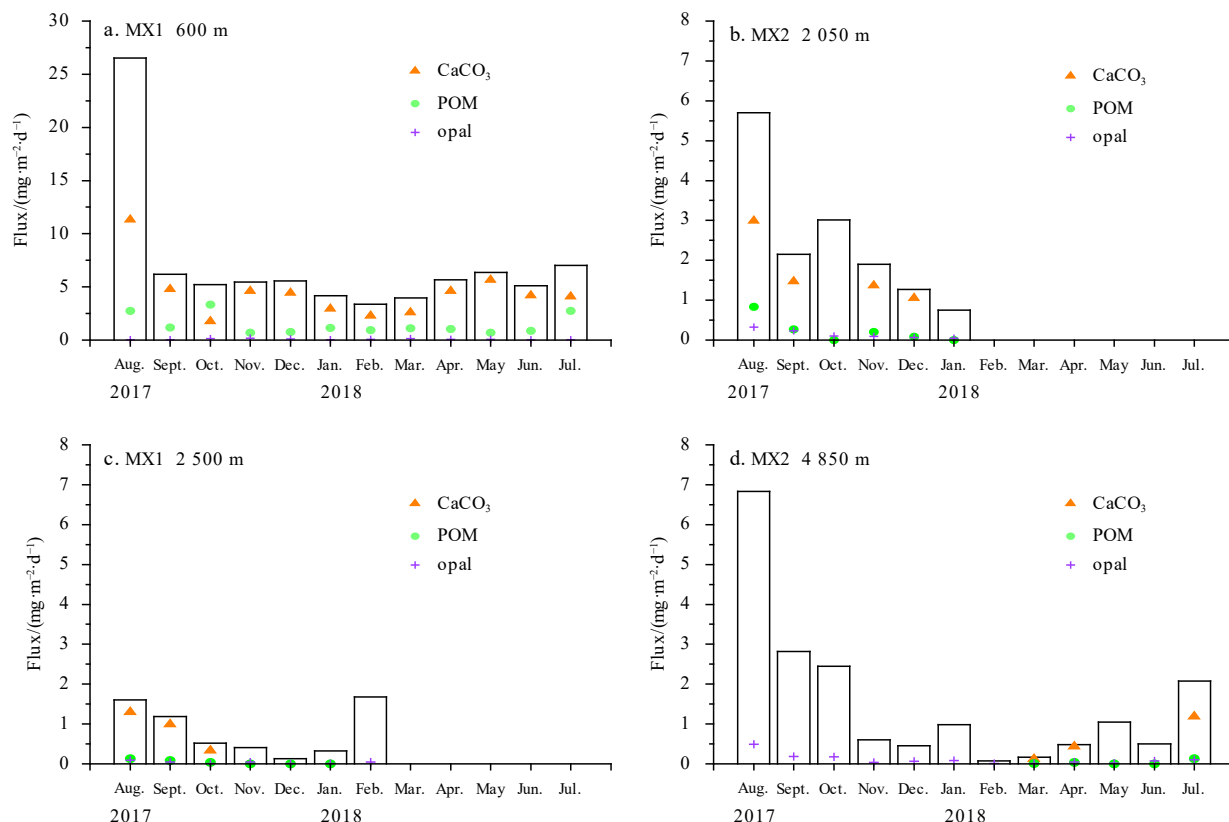


Fig. 4. Settling particle fluxes of total mass, CaCO₃, particulate organic matter (POM) and opal at different depths (the column represents total mass flux).

Table 3. Fluxes of total mass, total carbon (TC), total nitrogen (TN), particulate organic carbon (POC), opal and CaCO₃ collected by sediment trap

Site-layer	Cup No.	Time	Duration/d	Total mass flux/ (mg·m ⁻² ·d ⁻¹)	TC flux/ (mg·m ⁻² ·d ⁻¹)	TN flux/ (mg·m ⁻² ·d ⁻¹)	POC flux/ (mg·m ⁻² ·d ⁻¹)	Opal flux/ (mg·m ⁻² ·d ⁻¹)	CaCO ₃ flux/ (mg·m ⁻² ·d ⁻¹)	
MX1 600 m	2017444-3	August, 2017	30	26.52	2.89	0.224 7	1.53	0.04	11.33	
	2017444-4	September, 2017	30	6.18	1.24	0.142 8	0.66	0.02	4.78	
	2017444-5	October, 2017	30	5.20	2.07	0.140 5	1.85	0.13	1.77	
	2017444-6	November, 2017	30	5.45	0.94	0.077 5	0.38	0.19	4.64	
	2017444-7	December, 2017	30	5.56	0.95	0.077 6	0.42	0.09	4.45	
	2017444-8	January, 2018	30	4.18	0.98	0.110 3	0.63	0.05	2.94	
	2017444-9	February, 2018	30	3.36	0.79	0.088 8	0.52	0.06	2.28	
	2017444-10	March, 2018	30	3.96	0.93	0.155 5	0.62	0.15	2.59	
	2017444-11	April, 2018	30	5.68	1.12	0.110 4	0.57	0.06	4.61	
	2017444-12	May, 2018	30	6.37	1.07	0.068 0	0.39	0.07	5.65	
	2017444-13	June, 2018	30	5.10	1.00	0.094 3	0.49	0.03	4.21	
	2017444-14	July, 2018	23	7.04	2.02	0.219 5	1.53	0.04	4.10	
	MX1 2 500 m	2017443-3	August, 2017	30	1.60	0.23	0.012 8	0.07	0.10	1.30
		2017443-4	September, 2017	30	1.19	0.17	0.008 4	0.05	0.05	0.99
2017443-5		October, 2017	30	0.52	0.06	0.002 6	0.02	0.01	0.34	
2017443-6		November, 2017	30	0.41	0.07	0.012 8	–	0.05	–	
2017443-7		December, 2017	30	0.13	0.02	0.001 4	–	0.01	–	
2017443-8		January, 2018	30	0.33	0.04	0.001 9	–	0.01	–	
2017443-9		February, 2018	30	1.68	0.23	0.009 2	–	0.05	–	
2017443-10		March–July, 2018	143	3.12	0.44	0.018 7	0.12	0.14	2.57	
MX2 2 050 m		2017442-3	August, 2017	30	5.70	0.82	0.039 1	0.46	0.42	2.99
		2017442-4	September, 2017	30	2.15	0.33	0.018 9	0.15	0.23	1.47
	2017442-5	October, 2017	30	3.02	0.42	0.023 2	–	0.10	–	
	2017442-6	November, 2017	30	1.90	0.28	0.012 0	0.11	0.09	1.37	
	2017442-7	December, 2017	30	1.27	0.17	0.005 0	0.04	0.06	1.05	
	2017442-8	January, 2018	30	0.75	0.11	0.006 8	–	0.04	–	
	2017442-9	February–July, 2018	173	1.33	0.21	0.012 4	0.07	0.04	1.13	
	MX2 4 850 m	2017441-3	August, 2017	30	6.83	0.96	0.058 4	–	0.49	–
		2017441-4	September, 2017	30	2.82	0.38	0.017 4	–	0.19	–
2017441-5		October, 2017	30	2.45	0.33	0.017 5	–	0.18	–	
2017441-6		November, 2017	30	0.60	0.08	0.003 5	–	0.04	–	
2017441-7		December, 2017	30	0.45	0.07	0.004 4	–	0.06	–	
2017441-8		January, 2018	30	0.98	0.14	0.007 5	–	0.09	–	
2017441-9		February, 2018	30	0.07	–	–	–	0.01	–	
2017441-10		March, 2018	30	0.17	0.02	0.000 7	0.01	0.01	0.12	
2017441-11		April, 2018	30	0.48	0.07	0.003 6	0.02	0.01	0.43	
2017441-12		May, 2018	30	1.05	0.16	0.008 3	–	0.02	–	
2017441-13		June, 2018	30	0.50	0.08	0.006 6	–	0.07	–	
2017441-14		July, 2018	23	2.08	0.22	0.009 5	0.07	0.10	1.18	

Note: – represents data unavailable due to insufficient sample volume for measurement.

is characteristic of $C_{\text{org}}/C_{\text{inorg}}$ and $B_{\text{Si}}/C_{\text{inorg}}$ of <1. The sinking particles were rich in CaCO₃ in Niulang Guyot area, with an average of >70%. It was consistent with that Carbonate Ocean entailed 80% of the ocean between the North Pacific polar front and the Antarctic polar front (Honjo et al., 2008).

In the upper ocean, sinking mass fluxes and composition tend to be mediated by “swimmer”, as vertical migration of swimming animals and plankton would lead to significant changes in fluxes and it should not be considered as a part of the passively sinking flux (Michaels et al., 1990; Steinberg et al., 1998). We found biological residues (e.g., copepods) in some samples at 600 m before treatment. There was almost no correlation between each component and TMF. In contrast, fluxes of POC and CaCO₃ below 2 000 m were significantly correlated with TMF ($r=0.99$, $P<0.02$) (Figs 6a, b). Below 1 500 m, zooplankton had little impact on vertical transport of fluxes (Honjo et al.,

2008). Dissolution and mineralization were two main factors affecting the POC and CaCO₃. POC decreased with depth. CaCO₃ first increased with depth due to decomposition of organic matters and then decreased because of CaCO₃ dissolution (Fig. 6b).

The TMF of 2.57 g/(m²·a) at 600 m lies within a range of flux variation of 0.77–6.35 g/(m²·a) reported elsewhere (Kempe and Knaack, 1996; Kim et al., 2014, 2018), but it is far lower than those in the equatorial region (1.46–13.87 g/(m²·a)) and the western Pacific transition region (10.5–16.8 g/(m²·a)) (Kempe and Knaack, 1996; Mohiuddin et al., 2002, 2004). Regional differences in settling particle flux were caused by primary productivity, which was closely related to the concentration of surface chlorophyll *a* (Kim et al., 2018). Messié and Radenac (2006) reported distinct latitudinal variations of chlorophyll *a* concentration in the surface ocean, with a higher concentration (>0.2 mg/m³) in the equatorial zone of the West Pacific Ocean and a lower value

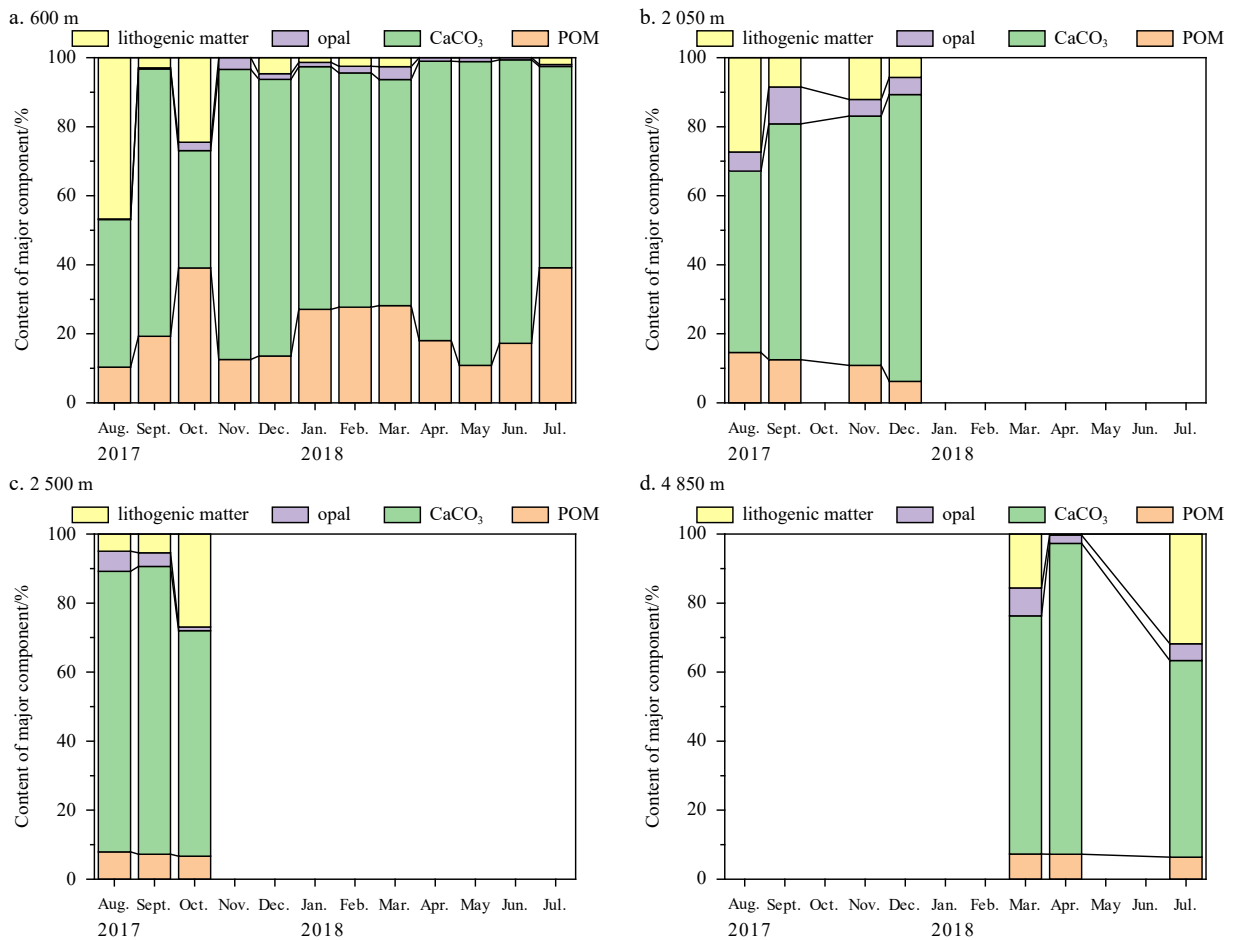


Fig. 5. Contents of major components (CaCO_3 , particulate organic matter (POM), opal and lithogenic matter) at different depths from August 2017 to July 2018 (only samples with complete data were displayed).

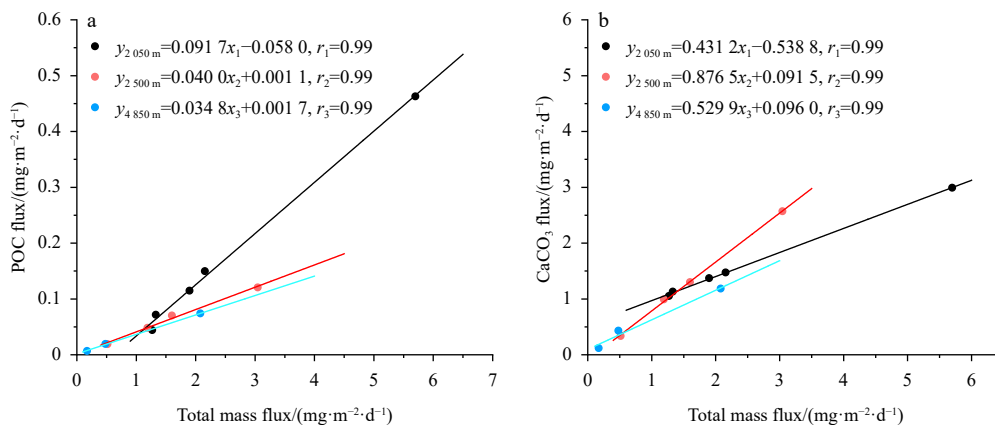


Fig. 6. Relationships between particulate organic carbon (POC), CaCO_3 and total mass flux.

(<0.1 mg/m^3) in the SONP. The remarkably low chlorophyll *a* (Fig. 2) in the seamount area was in agreement with our flux data. The export flux of POC was proportional to TMF across the boundary between the euphotic and bathypelagic zones (Schindler, 1975). Constrained by such low TMF, the export of biogenic components such as POC to deep ocean was even lower than warm pool area (Kempe and Knaack, 1996), which was known for its lowest flux (Honjo et al., 2008).

TMFs of MX1 and MX2 exhibited similar seasonal changes al-

though they were located in different geographical locations ($r > 0.90$, $P < 0.01$, statistically results between 600 m, 2 050 m and 4 850 m). The flux variation usually reflected the changes in the primary production of the upper water and was closely related to the growth of plankton. From January 2017 to December 2018, the content of chlorophyll *a* in the surface layer fluctuated around 0.05 mg/m^3 , except a high value of 0.09 mg/m^3 at high temperature (Fig. 2), reflecting an ecosystem dominated by picoplankton and low seasonality, with relatively low and con-

stant rates of primary production (Buesseler et al., 2007; Brown et al., 2022). Thus, TMF was dominated by the calcareous ballast which was also confirmed by a large number of planktonic foraminiferal tests in samples at 600 m collected in August besides the changes of primary production. Calcite is one of the heaviest bio-minerals in seawater and is more resistant to dissolution in sea water than other pelagic biominerals, including biogenic opal aragonite and magnesium-rich calcite (Milliman, 1974). Previous studies showed a calcite-dominated TMF in the subtropical Pacific Ocean (Honjo et al., 1995; Kim et al., 2011, 2017), and dense planktonic foraminifera shells comprised from 20% to 70% of CaCO_3 flux with shell sizes mostly larger than 125 μm (Mohiuddin et al., 2002, 2004; Kim et al., 2010). The settling rate of large planktonic foraminifera (>125 μm) in laboratory experiments ranged between 320 m/d and 1 270 m/d (Takahashi and Be, 1984). Settling particles, most of which were probably planktonic foraminifera aggregates, would sink rapidly to the deep sea and retained well in the traps. At 4 850 m, CaCO_3 still accounted for 57% to 90% and foraminiferal tests appeared in almost all samples. Like TMF, the number of foraminifera was the highest in August 2017 and the lowest in February 2018. The peak and valley values at the shallow depth were consistent with the deep layer, without temporal offsets, suggesting the residence time of settling particles shorter than one month time-series resolution during most of the period.

Particles rich in foraminiferal tests that settled on the seamount were more likely to accumulate at the hillside than the top due to the topography and currents. The dissolution of CaCO_3 increased with depth and more CaCO_3 dissolved at the hillside. So CaCO_3 content in surface sediment reduced from 82% of the top (20.40°N, 160.78°E, 1 800 m) to 64% of the hillside (20.52°N, 161.07°E, 2 486 m), while the organic carbon increased from 0.03% to 0.14%, resulting in an increase in the abundance of meiobenthos by 7 times (from 0.194 ind./m² to 1.515 ind./m²).

The sinking materials would gradually decrease due to the mineralization of organic matter and the dissolution of carbonate with increasing depth. However, in August and September, the TMFs at 4 850 m were higher than that at 2 050 m, with an increase of up to 20%. In general, the decrease of current velocity and the solidification of aggregates with depth would lead to the increase in capture efficiency (Scholten et al., 2001; Yu et al., 2001). Treppke et al. (1996) found that the resuspended sediments would result in an increase in fluxes. Hwang et al. (2010) suggested that the resuspension of sediment and its lateral transport was widespread and was an important component of oceanic carbon cycle. The velocity of the adjacent layers where the trap was located at 4 920 m was much higher than at 1 846 m (Figs 3c, d), especially in August and September. Therefore, it can be speculated that the flux anomaly may be caused by resuspension of sediment and its lateral transport.

The flux at 600 m layer in August was anomaly higher than that in other months (4 times of that in July and September), and ballast was as high as 47%. In the open ocean, lithic matter usually came from aerosol particles, while the crust aerosol ions played an important role (Tegen and Fung, 1994; Mahowald et al., 1999). Generally, the abundant supply came from the important dry land and desert region near the upper wind side of the ocean edge, but the MX1 site was far away from the continents, and was unlikely to be affected by atmospheric transport dust. Another important reason for the anomaly increase of flux was the earthquake, which usually occurred in the slope area or trench area, the mass flux can increase to 9 times more than that before earthquake (Itou and Noriki, 1997). MX1 was located on

the hillside of Niulang Guyot and the geographical conditions were similar to the land slope, however the 600 m trap was far away from the mountain top which could avoid the earthquake. However, further studies are needed for the abnormal flux at 600 m in August.

4.2 Attenuation of sinking POC flux

The biological carbon pump, which transports POC from the surface to the deep ocean, plays an important role in regulating atmospheric carbon dioxide (CO_2) concentrations (Marsay et al., 2015). Therefore, the deep-sea transport of POC is of great concern. POC flux decreases with depth, namely, POC flux attenuation, is a product of remineralization rate of organic materials and sinking velocity of the POC-containing particles. Numerous studies endeavored to describe the process of sinking POC flux attenuation as relatively simple mathematical forms (Suess, 1980; Armstrong et al., 2001; Lutz et al., 2002; Boyd and Trull, 2007), with perhaps the most commonly used being a power law equation:

$$F_z = F_{z_0} (z/z_0)^{-b}, \quad (4)$$

where F_z was the flux at depth z , normalized to flux at some reference depth z_0 , and b was the coefficient of flux attenuation (Martin et al., 1987). Additionally, the degree of POC flux attenuation can be expressed as transfer efficiency based on sediment trap data (Buesseler et al., 2007). Due to the lack of samples, POC fluxes during some periods cannot be measured, which made it difficult to estimate the POC attenuation. However, in the deep ocean, we found that there was a significant positive correlation between POC flux and TMF ($r \geq 0.99$, $P < 0.01$) which provided a tool to estimate the annual average POC flux. The calculated POC fluxes at 2 050 m, 2 500 m, and 4 850 m were 0.17 mg/(m²·d), 0.07 mg/(m²·d), and 0.05 mg/(m²·d), respectively. Compared with 600 m (0.78 mg/(m²·d), the transport efficiency of POC at 2 050 m, 2 500 m and 4 850 m was 22%, 9% and 7%, respectively. The attenuation of POC mainly occurred in twilight zone (water depth between transparent zone and 1 000 m). The estimated transport efficiency in the upper water was similar to the 20% observed at Station ALOHA in the North Pacific subtropical circulation, but far lower than that observed at Station K2 (46%–55%) in the Northwest Pacific subarctic circulation.

POC fluxes at this area were fitted to Eq. (4) to calculate b , yielding values of 1.34, which was consistent with what Buesseler et al. (2007) found $b=1.33$. The monthly values were also captured by the regional variation range of deep-sea b value (0.6–2.0) (Berelson, 2001; Francois et al., 2002), but much higher than 0.86 (Martin et al., 1987) derived from several locations of the eastern North Pacific Ocean, reflecting the larger percentage decrease of POC flux in the upper water at Niulang Guyot area (Fig. 7). From August 2017 to January 2018, monthly b values showed an increase before December 2017 and then decreased at January 2018. Resuspension of sediment may lead to an increase of TMF near bottom, which would increase the POC flux, resulting in a decrease in b value. In August, assuming that the increment of TMF caused by resuspension sediment accounts for 20% and its organic carbon content was about 0.3%, the calibrated b value was 1.09, the variation of b value caused by sediment resuspension was only 0.01. The relative lower b values of August and September indicated a relatively higher POC export efficiency, further demonstrating the calcareous ballasts in the upper water dominates POC flux. Proper quantification of the export and re-

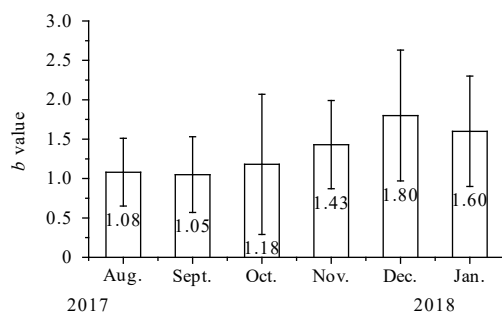


Fig. 7. Monthly b value chart with error bar from August 2017 to January 2018.

mineralization of POC in ocean carbon cycle models and corresponding changes in POC/PIC (particulate inorganic carbon) content ratios were important (Howard et al., 2006). Modeling results suggested that the selection of POC parameters were very sensitive to the model output results, and the use of regionally variable POC flux parameterization could minimize the difference between simulated and observed carbon tracers (PO_4 , Alk*) and model-data differences of POC fluxes (Howard et al., 2006). Our result improved the accuracy of regional biochemical model outcome in subtropical oligotrophic zone.

The regional difference in transfer efficiency was attributed to the phytoplankton community structure (Kim et al., 2018). The diatom-dominated ecosystem station (K2) had a higher transfer POC efficiency than Station ALOHA (Honda, 2003). The study area was located in the oligotrophic Northwest Pacific Ocean where the mean state of ecosystem was characterized by a dominance of small picophytoplankton with tightly balanced rates of growth and mortality (Browning et al., 2022) and nitrogen fixation contributes up to half of export production (Karl et al., 1997). Kitajima et al. (2009) showed that the N_2 fixation was primarily ascribed to $<10 \mu\text{m}$ diazotrophs—nanoplanktonic cyanobacteria, line with those previous studies conducted in various part of oligotrophic ocean (Zehr et al., 2001; Dore et al., 2002; Montoya et al., 2004). Researches also showed that phytoplankton productivity and POC sinking flux were controlled mainly by cyanobacteria *Prochlorococcus* in SONP (Karl et al., 1996; Partensky et al., 1999; Moore et al., 2002). Our research on photosynthetic pigments indicated that the first dominant group of phytoplankton biomass was *prochlorococcus* in August 2017. The semi-permeable protein shell of cyanobacteria was prone to being mineralized than diatom phytoplankton, therefore most of POC were remineralized in oxygen minimum zone. Water temperature was another important factor affecting the attenuation of POC, and the remineralization of POC in warm waters would become shallower (Marsay et al., 2015). Warming the Northwest Pacific Ocean (Balaguru et al., 2016) would lead to ocean acidification, leading to less calcite ballasting and lower transfer efficiency of sinking POC to the deep sea.

5 Conclusions

A one-year-long observation by four sediment traps was used to investigate seasonal variations of settling particles and their composition in Niulang Guyot area of the oligotrophic western Pacific Ocean. TMF at each layer had similar seasonal pattern, higher in summer and lower in winter. The peak and valley fluxes in the upper matched those in the deep, indicating that particles sank from 600 m to 4 850 m within a 30-d period without significant temporal delay. Fast settling rate of sinking particles caused

by calcium carbonate ballast would be beneficial to the export of POC, but only a small proportion of POM was transported to the deep sea, which may be associated with cyanobacteria-dominated phytoplankton. Continued surface water warming would likely have a profound impact on ocean acidification in the Northwest Pacific Ocean, possibly affecting the biological pump, and local seamount environment such as topography and current could have an important impact on the carbon flux in regional area. Therefore, more observations based on moorings are needed in the further research of biological pump and optimization of regional biological models in seamount area.

Acknowledgements

We would like to thank the crew of R/V *Xiangyanghong 03* for their support and help.

References

- Armstrong R A, Lee C, Hedges J I, et al. 2001. A new, mechanistic model for organic carbon fluxes in the ocean based on the quantitative association of POC with ballast minerals. *Deep-Sea Research Part II: Topical Studies in Oceanography*, 49(1-3): 219–236, doi: [10.1016/S0967-0645\(01\)00101-1](https://doi.org/10.1016/S0967-0645(01)00101-1)
- Balaguru K, Foltz G R, Leung L R, et al. 2016. Global warming-induced upper-ocean freshening and the intensification of super typhoons. *Nature Communications*, 7: 13670, doi: [10.1038/ncomms13670](https://doi.org/10.1038/ncomms13670)
- Berelson W M. 2001. The flux of particulate organic carbon into the ocean interior: a comparison of four U. S. JGOFS regional studies. *Oceanography*, 14(4): 59–67, doi: [10.5670/oceanog.2001.07](https://doi.org/10.5670/oceanog.2001.07)
- Boyd P W, Trull T W. 2007. Understanding the export of biogenic particles in oceanic waters: is there consensus?. *Progress in Oceanography*, 72(4): 276–312, doi: [10.1016/j.pocean.2006.10.007](https://doi.org/10.1016/j.pocean.2006.10.007)
- Browning T J, Liu Xin, Zhang Ruifeng, et al. 2022. Nutrient co-limitation in the subtropical Northwest Pacific. *Limnology and Oceanography Letters*, 7(1): 52–61, doi: [10.1002/lo.12025](https://doi.org/10.1002/lo.12025)
- Buesseler K O, Lamborg C H, Boyd P W, et al. 2007. Revisiting carbon flux through the ocean's twilight zone. *Science*, 316(5824): 567–570, doi: [10.1126/science.1137959](https://doi.org/10.1126/science.1137959)
- Buesseler K O, Trull T W, Steinberg D K, et al. 2008. VERTIGO (Vertical Transport in the Global Ocean): a study of particle sources and flux attenuation in the North Pacific. *Deep-Sea Research Part II: Topical studies in Oceanography*, 55(14–15): 1522–1539, doi: [10.1016/j.dsr2.2008.04.024](https://doi.org/10.1016/j.dsr2.2008.04.024)
- Dore J E, Brum J R, Tupas L M, et al. 2002. Seasonal and interannual variability in sources of nitrogen supporting export in the oligotrophic subtropical North Pacific Ocean. *Limnology and Oceanography*, 47(6): 1595–1607, doi: [10.4319/lo.2002.47.6.1595](https://doi.org/10.4319/lo.2002.47.6.1595)
- Dower J F, Mackas D L. 1996. "Seamount effects" in the zooplankton community near Cobb Seamount. *Deep-Sea Research Part I: Oceanographic Research Papers*, 43(6): 837–858, doi: [10.1016/0967-0637\(96\)00040-4](https://doi.org/10.1016/0967-0637(96)00040-4)
- Ducklow H W, Doney S C, Steinberg D K. 2009. Contributions of long-term research and time-series observations to marine ecology and biogeochemistry. *Annual Review of Marine Science*, 1: 279–302, doi: [10.1146/annurev.marine.010908.163801](https://doi.org/10.1146/annurev.marine.010908.163801)
- Emerson S, Quay P, Karl D, et al. 1997. Experimental determination of the organic carbon flux from open-ocean surface waters. *Nature*, 389(6654): 951–954, doi: [10.1038/40111](https://doi.org/10.1038/40111)
- Francois R, Honjo S, Krishfield R, et al. 2002. Factors controlling the flux of organic carbon to the bathypelagic zone of the ocean. *Global Biogeochemical Cycles*, 16(4): 1087, doi: [10.1029/2001gb001722](https://doi.org/10.1029/2001gb001722)
- Gao Meng, Huang Baoqi, Liu Zhifei, et al. 2020. Observations of marine snow and fecal pellets in a sediment trap mooring in the northern South China Sea. *Acta Oceanologica Sinica*, 39(3): 141–147, doi: [10.1007/s13131-020-1561-9](https://doi.org/10.1007/s13131-020-1561-9)
- Harada N, Handa N, Harada K, et al. 2001. Alkenones and particulate

- fluxes in sediment traps from the central equatorial Pacific. *Deep-Sea Research Part I: Oceanographic Research Papers*, 48(3): 891–907, doi: [10.1016/S0967-0637\(00\)00077-7](https://doi.org/10.1016/S0967-0637(00)00077-7)
- Haskell II W Z, Berelson W M, Hammond D E, et al. 2013. Particle sinking dynamics and POC fluxes in the Eastern Tropical South Pacific based on ²³⁴Th budgets and sediment trap deployments. *Deep-Sea Research Part I: Oceanographic Research Papers*, 81: 1–13, doi: [10.1016/j.dsr.2013.07.001](https://doi.org/10.1016/j.dsr.2013.07.001)
- Henson S A, Sanders R, Madsen E. 2012. Global patterns in efficiency of particulate organic carbon export and transfer to the deep ocean. *Global Biogeochemical Cycles*, 26(1): GB1028, doi: [10.1029/2011GB004099](https://doi.org/10.1029/2011GB004099)
- Hernández-Ávila I, Pech D, Ocaña F A, et al. 2021. Shelf and deep-water benthic macrofauna assemblages from the western Gulf of Mexico: temporal dynamics and environmental drivers. *Marine Environmental Research*, 165: 105241, doi: [10.1016/j.marenvres.2020.105241](https://doi.org/10.1016/j.marenvres.2020.105241)
- Honda M C. 2003. Biological pump in northwestern North Pacific. *Journal of Oceanography*, 59(5): 671–684, doi: [10.1023/B:JOCE.0000009596.57705.0c](https://doi.org/10.1023/B:JOCE.0000009596.57705.0c)
- Honjo S, Dymond J, Collier R, et al. 1995. Export production of particles to the interior of the equatorial Pacific Ocean during the 1992 EqPac experiment. *Deep-Sea Research Part II: Topical Studies in Oceanography*, 42(2–3): 831–870, doi: [10.1016/0967-0645\(95\)00034-n](https://doi.org/10.1016/0967-0645(95)00034-n)
- Honjo S, Manganini S J, Krishfield R A, et al. 2008. Particulate organic carbon fluxes to the ocean interior and factors controlling the biological pump: a synthesis of global sediment trap programs since 1983. *Progress in Oceanography*, 76(3): 217–285, doi: [10.1016/j.pocean.2007.11.003](https://doi.org/10.1016/j.pocean.2007.11.003)
- Howard M T, Winguth A M E, Klaas C, et al. 2006. Sensitivity of ocean carbon tracer distributions to particulate organic flux parameterizations. *Global Biogeochemical Cycles*, 20(3): GB3011, doi: [10.1029/2005GB002499](https://doi.org/10.1029/2005GB002499)
- Hwang J, Druffel E R M, Eglinton T I. 2010. Widespread influence of resuspended sediments on oceanic particulate organic carbon: insights from radiocarbon and aluminum contents in sinking particles. *Global Biogeochemical Cycles*, 20(4): GB4016, doi: [10.1029/2010GB003802](https://doi.org/10.1029/2010GB003802)
- Ito M, Noriki S. 1997. Temporal changes of particulate flux observed in the northern Japan trench. In: Tsunogai S, ed. *Biogeochemical Processes in the North Pacific*. Tokyo: Japan Marine Science Foundation, 262–269
- Karl D M, Christian J R, Dore J E, et al. 1996. Seasonal and interannual variability in primary production and particle flux at Station ALOHA. *Deep-Sea Research Part II: Topical Studies in Oceanography*, 43(2–3): 539–568, doi: [10.1016/0967-0645\(96\)00002-1](https://doi.org/10.1016/0967-0645(96)00002-1)
- Karl D, Letelier R, Tupas L, et al. 1997. The role of nitrogen fixation in biogeochemical cycling in the subtropical North Pacific Ocean. *Nature*, 388(6642): 533–538, doi: [10.1038/41474](https://doi.org/10.1038/41474)
- Kempe S, Knaack H. 1996. Vertical particle flux in the western Pacific below the North Equatorial Current and the Equatorial Counter Current. In: Ittekkot V, Schäfer P, Honjo S, et al., eds. *Particle Flux in the Ocean*, SCOPE Report 57. New York: John Wiley & Sons, Chichester: 313–323
- Kim H J, Hyeong K, Park J Y, et al. 2014. Influence of Asian monsoon and ENSO events on particle fluxes in the western subtropical Pacific. *Deep-Sea Research Part I: Oceanographic Research Papers*, 90: 139–151, doi: [10.1016/j.dsr.2014.05.002](https://doi.org/10.1016/j.dsr.2014.05.002)
- Kim H J, Hyeong K, Yoo C M, et al. 2010. Seasonal variations of particle fluxes in the northeastern equatorial Pacific during normal and weak El Niño periods. *Geosciences Journal*, 14(4): 415–422, doi: [10.1007/s12303-010-0035-z](https://doi.org/10.1007/s12303-010-0035-z)
- Kim H J, Hyeong K S, Yoo C M, et al. 2011. Temporal and spatial variations of sinking-particle fluxes in the northwestern subtropical Pacific. *Ocean and Polar Research (in Korean)*, 33(3): 385–395, doi: [10.4217/OPR.2011.33.3.385](https://doi.org/10.4217/OPR.2011.33.3.385)
- Kim D, Jeong J H, Kim T W, et al. 2017. The reduction in the biomass of cyanobacterial N₂ fixer and the biological pump in the northwestern Pacific Ocean. *Scientific Reports*, 7: 41810, doi: [10.1038/srep41810](https://doi.org/10.1038/srep41810)
- Kim H J, Kim J, Kim D, et al. 2018. Sinking particle flux in the subtropical oligotrophic northwestern Pacific from a short-term sediment trap experiment. *Ocean Science Journal*, 53(2): 395–403, doi: [10.1007/s12601-018-0025-z](https://doi.org/10.1007/s12601-018-0025-z)
- Kitajima S, Furuya K, Hashihama F, et al. 2009. Latitudinal distribution of diazotrophs and their nitrogen fixation in the tropical and subtropical western North Pacific. *Limnology and Oceanography*, 54(2): 537–547, doi: [10.4319/lo.2009.54.2.0537](https://doi.org/10.4319/lo.2009.54.2.0537)
- Kwak J H, Han E, Hwang J, et al. 2017. Flux and stable C and N isotope composition of sinking particles in the Ulleung Basin of the East/Japan Sea. *Deep-Sea Research Part II: Topical Studies in Oceanography*, 143: 62–72, doi: [10.1016/j.dsr2.2017.03.014](https://doi.org/10.1016/j.dsr2.2017.03.014)
- Leduc D, Nodder S D, Pinkerton M, et al. 2020. Benthic metabolism on Chatham Rise, New Zealand continental margin: temporal and spatial variability, and relationships with macrofauna and environmental factors. *Deep-Sea Research Part I: Oceanographic Research Papers*, 159: 103239, doi: [10.1016/j.dsr.2020.103239](https://doi.org/10.1016/j.dsr.2020.103239)
- Li Hongliang, Wiesner M G, Chen Jianfang, et al. 2017. Long-term variation of mesopelagic biogenic flux in the central South China Sea: impact of monsoonal seasonality and mesoscale eddy. *Deep-Sea Research Part I: Oceanographic Research Papers*, 126: 62–72, doi: [10.1016/j.dsr.2017.05.012](https://doi.org/10.1016/j.dsr.2017.05.012)
- Lutz M, Dunbar R, Caldeira K. 2002. Regional variability in the vertical flux of particulate organic carbon in the ocean interior. *Global Biogeochemical Cycles*, 16(3): 1037, doi: [10.1029/2000GB001383](https://doi.org/10.1029/2000GB001383)
- Ma Qiang, Chen Min, Qiu Yusheng, et al. 2005. Regional estimates of POC export flux derived from thorium-234 in the western Arctic Ocean. *Acta Oceanologica Sinica*, 24(6): 97–108
- Mahowald N, Kohfeld K, Hansson M, et al. 1999. Dust sources and deposition during the last glacial maximum and current climate: a comparison of model results with paleodata from ice cores and marine sediments. *Journal of Geophysical Research: Atmospheres*, 104(D13): 15895–15916, doi: [10.1029/1999JD900084](https://doi.org/10.1029/1999JD900084)
- Marsay C M, Sanders R J, Henson S A, et al. 2015. Attenuation of sinking particulate organic carbon flux through the mesopelagic ocean. *Proceedings of the National Academy of Sciences of the United States of America*, 112(4): 1089–1094, doi: [10.1073/pnas.1415311112](https://doi.org/10.1073/pnas.1415311112)
- Martin J H, Knauer G A, Karl D M, et al. 1987. VERTEX: carbon cycling in the northeast Pacific. *Deep-Sea Research Part A: Oceanographic Research Papers*, 34(2): 267–285, doi: [10.1016/0198-0149\(87\)90086-0](https://doi.org/10.1016/0198-0149(87)90086-0)
- McClain C R, Hardy S M. 2010. The dynamics of biogeographic ranges in the deep sea. *Proceedings of the Royal Society B: Biological Sciences*, 277(1700): 3533–3546, doi: [10.1098/rspb.2010.1057](https://doi.org/10.1098/rspb.2010.1057)
- Messié M, Radenac M H. 2006. Seasonal variability of the surface chlorophyll in the western tropical Pacific from SeaWiFS data. *Deep-Sea Research Part I: Oceanographic Research Papers*, 53(10): 1581–1600, doi: [10.1016/j.dsr.2006.06.007](https://doi.org/10.1016/j.dsr.2006.06.007)
- Michaels A F, Silver M W, Gowing M M, et al. 1990. Cryptic zooplankton “swimmers” in upper ocean sediment traps. *Deep-Sea Research Part A: Oceanographic Research Papers*, 37(8): 1285–1296, doi: [10.1016/0198-0149\(90\)90043-U](https://doi.org/10.1016/0198-0149(90)90043-U)
- Milliman J D. 1974. *Marine Carbonates*. Berlin: Springer-Verlag, 1–375
- Mohiuddin M M, Nishimura A, Tanaka Y, et al. 2002. Regional and interannual productivity of biogenic components and planktonic foraminiferal fluxes in the northwestern Pacific Basin. *Marine Micropaleontology*, 45(1): 57–82, doi: [10.1016/S0377-8398\(01\)00045-7](https://doi.org/10.1016/S0377-8398(01)00045-7)
- Mohiuddin M M, Nishimura A, Tanaka Y, et al. 2004. Seasonality of biogenic particle and planktonic foraminifera fluxes: Response to hydrographic variability in the Kuroshio Extension, northwestern Pacific Ocean. *Deep-Sea Research Part I: Oceanographic Research Papers*, 51(11): 1659–1683, doi: [10.1016/j.dsr.2004.06.002](https://doi.org/10.1016/j.dsr.2004.06.002)
- Montoya J P, Holl C M, Zehr J P, et al. 2004. High rates of N₂ fixation

- by unicellular diazotrophs in the oligotrophic Pacific Ocean. *Nature*, 430(7003): 1027–1031, doi: [10.1038/nature02824](https://doi.org/10.1038/nature02824)
- Moore L R, Post A F, Rocap G, et al. 2002. Utilization of different nitrogen sources by the marine cyanobacteria *Prochlorococcus* and *Synechococcus*. *Limnology and Oceanography*, 47(4): 989–996, doi: [10.4319/lo.2002.47.4.0989](https://doi.org/10.4319/lo.2002.47.4.0989)
- Mortlock R A, Froelich P N. 1989. A simple method for the rapid determination of biogenic opal in pelagic marine sediments. *Deep-Sea Research Part A. Oceanographic Research Papers*, 36(9): 1415–1426, doi: [10.1016/0198-0149\(89\)90092-7](https://doi.org/10.1016/0198-0149(89)90092-7)
- Müller P J, Suess E, AndréUngerer C. 1986. Amino acids and amino sugars of surface particulate and sediment trap material from waters of the Scotia Sea. *Deep-Sea Research Part A. Oceanographic Research Papers*, 33(6): 819–838, doi: [10.1016/0198-0149\(86\)90090-7](https://doi.org/10.1016/0198-0149(86)90090-7)
- Nowald N, Iversen M H, Fischer G, et al. 2015. Time series of *in-situ* particle properties and sediment trap fluxes in the coastal upwelling filament off Cape Blanc, Mauritania. *Progress in Oceanography*, 137: 1–11, doi: [10.1016/j.pocean.2014.12.015](https://doi.org/10.1016/j.pocean.2014.12.015)
- Partensky F, Blanchot J, Vulot D. 1999. Differential distribution and ecology of *Prochlorococcus* and *Synechococcus* in oceanic waters: a review. *Bulletin de l'Institut Océanographique*, 19: 457–475
- Priede I G, Froese R. 2013. Colonization of the deep sea by fishes. *Journal of Fish Biology*, 83(6): 1528–1550, doi: [10.1111/jfb.12265](https://doi.org/10.1111/jfb.12265)
- Ragueneau O, Savoye N, Del Amo Y, et al. 2005. A new method for the measurement of biogenic silica in suspended matter of coastal waters: using Si: Al ratios to correct for the mineral interference. *Continental Shelf Research*, 25(5–6): 697–710 doi: [10.1016/j.csr.2004.09.017](https://doi.org/10.1016/j.csr.2004.09.017)
- Ramaswamy V, Kumar B V, Parthiban G, et al. 1997. Lithogenic fluxes in the Bay of Bengal measured by sediment traps. *Deep-Sea Research Part I: Oceanographic Research Papers*, 44(5): 793–810, doi: [10.1016/S0967-0637\(96\)00117-3](https://doi.org/10.1016/S0967-0637(96)00117-3)
- Ran Lihua, Chen Jianfang, Wiesner M G, et al. 2015. Variability in the abundance and species composition of diatoms in sinking particles in the northern South China Sea: results from time-series moored sediment traps. *Deep-Sea Research Part II: Topical Studies in Oceanography*, 122: 15–24, doi: [10.1016/j.dsr2.2015.07.004](https://doi.org/10.1016/j.dsr2.2015.07.004)
- Rowden A A, Schlacher T A, Williams A, et al. 2010. A test of the seamount oasis hypothesis: seamounts support higher epibenthic megafaunal biomass than adjacent slopes. *Marine Ecology*, 31(S1): 95–106, doi: [10.1111/j.1439-0485.2010.00369.x](https://doi.org/10.1111/j.1439-0485.2010.00369.x)
- Schindler D W. 1975. Broecker, W. S. 1974. *Chemical oceanography*. Harcourt, Brace, Jovanovich, Inc., New York. 214 p. \$7.95. *Limnology and Oceanography*, 20(2): 299–300, doi: [10.4319/lo.1975.20.2.0299](https://doi.org/10.4319/lo.1975.20.2.0299)
- Scholten J C, Fietzke J, Vogler S, et al. 2001. Trapping efficiencies of sediment traps from the deep eastern North Atlantic: the ²³⁰Th calibration. *Deep-Sea Research Part II: Topical Studies in Oceanography*, 48(10): 2383–2408, doi: [10.1016/S0967-0645\(00\)00176-4](https://doi.org/10.1016/S0967-0645(00)00176-4)
- Steinberg D K, Pilskaln C H, Silver M W. 1998. Contribution of zooplankton associated with detritus to sediment trap 'swimmer' carbon in Monterey Bay, California, USA. *Marine Ecology Progress Series*, 164: 157–166, doi: [10.3354/meps164157](https://doi.org/10.3354/meps164157)
- Suess E. 1980. Particulate organic carbon flux in the oceans-surface productivity and oxygen utilization. *Nature*, 288(5788): 260–263, doi: [10.1038/288260a0](https://doi.org/10.1038/288260a0)
- Takahashi K, Be A W H. 1984. Planktonic foraminifera: factors controlling sinking speeds. *Deep-Sea Research Part A. Oceanographic Research Papers*, 31(12): 1477–1500, doi: [10.1016/0198-0149\(84\)90083-9](https://doi.org/10.1016/0198-0149(84)90083-9)
- Tegen I, Fung I. 1994. Modeling of mineral dust in the atmosphere: SOURCES, transport, and optical thickness. *Journal of Geophysical Research: Atmospheres*, 99(D11): 22897–22914, doi: [10.1029/94JD01928](https://doi.org/10.1029/94JD01928)
- Treppke U F, Lange C B, Wefer G. 1996. Vertical fluxes of diatoms and silicoflagellates in the eastern equatorial Atlantic, and their contribution to the sedimentary record. *Marine Micropaleontology*, 28(1): 73–96, doi: [10.1016/0377-8398\(95\)00046-1](https://doi.org/10.1016/0377-8398(95)00046-1)
- Turnewitsch R, Dumont M, Kiriakoulakis K, et al. 2016. Tidal influence on particulate organic carbon export fluxes around a tall seamount. *Progress in Oceanography*, 149: 189–213, doi: [10.1016/j.pocean.2016.10.009](https://doi.org/10.1016/j.pocean.2016.10.009)
- Wei Bingbing, Li Jiangtao, Zhang Li, et al. 2015. Application of ²³⁴Th/²³⁸U disequilibrium to the study of marine particle cycling. *Marine Geology Frontiers*, 31(11): 1–9, doi: [10.16028/j.1009-2722.2015.11001](https://doi.org/10.16028/j.1009-2722.2015.11001)
- Wilks J V, Rigual-Hernández A S, Trull T W, et al. 2017. Biogeochemical flux and phytoplankton succession: a year-long sediment trap record in the Australian sector of the Subantarctic Zone. *Deep-Sea Research Part I: Oceanographic Research Papers*, 121: 143–159, doi: [10.1016/j.dsr.2017.01.001](https://doi.org/10.1016/j.dsr.2017.01.001)
- Yang Yongliang, Han Xu, Kusakabe M. 2004. POC fluxes from euphotic zone estimated from ²³⁴Th deficiency in winter in the northwestern North Pacific Ocean. *Acta Oceanologica Sinica*, 23(1): 135–148
- Yesson C, Clark M R, Taylor M L, et al. 2011. The global distribution of seamounts based on 30 arc seconds bathymetry data. *Deep-Sea Research Part I: Oceanographic Research Papers*, 58(4): 442–453, doi: [10.1016/j.dsr.2011.02.004](https://doi.org/10.1016/j.dsr.2011.02.004)
- Yokoi N, Abe Y, Kitamura M, et al. 2018. Comparisons between POC and zooplankton swimmer flux from sediment traps in the subarctic and subtropical North Pacific. *Deep-Sea Research Part I: Oceanographic Research Papers*, 133: 19–26, doi: [10.1016/j.dsr.2018.01.003](https://doi.org/10.1016/j.dsr.2018.01.003)
- Yu E F, Francois R, Bacon M P, et al. 2001. Trapping efficiency of bottom-tethered sediment traps estimated from the intercepted fluxes of ²³⁰Th and ²³¹Pa. *Deep-Sea Research Part I: Oceanographic Research Papers*, 48(3): 865–889, doi: [10.1016/s0967-0637\(00\)00067-4](https://doi.org/10.1016/s0967-0637(00)00067-4)
- Zehr J P, Waterbury J B, Turner P J, et al. 2001. Unicellular cyanobacteria fix N₂ in the subtropical North Pacific Ocean. *Nature*, 412(6847): 635–638, doi: [10.1038/35088063](https://doi.org/10.1038/35088063)
- Zhang Junlong, Xu Kuidong. 2013. Progress and prospects in seamount biodiversity. *Advances in Earth Science*, 28(11): 1209–1216